

Research on the Expression Pattern, Prognostic Value, and Immune Microenvironment Regulatory Mechanism of GLS Gene in Pan-cancer

Xinyao Li, Shijia Lu, Yufeng Nie, Jing Fang, Songyang Gao, Wenbo Qi, Keru Li, Tianle Zhang, Jinwen Sima*

North Henan Medical University, Xinxiang 453003, China

*Corresponding email: simajinwen@126.com

Abstract

This study systematically elucidates the central regulatory function of glutaminase (GLS) genes in pan-cancer contexts and their role in remodeling the tumor immune microenvironment. Through the integration and analysis of extensive pan-cancer datasets, it was revealed that GLS expression exhibits a highly cancer-specific pattern and is associated with a “double-edged sword” prognostic value, reflecting the cancer type’s dependence on the “ammonia death” threshold effect. The primary innovation of this research lies in demonstrating that GLS influence genomic stability through metabolism-epigenetic cross-dialogue, thereby driving unique immune microenvironment regulation. Specifically, GLS promote immune recognition while simultaneously inducing excessive ammonia-induced “ammonia death” of CD8⁺ T cells, leading to immune exhaustion. This mechanism has been corroborated by multiple algorithms across various cancer types. This study has for the first time established a precise intervention framework based on GLS expression: Targeting and inhibiting the GLS activity of high-expression cancer types or activating the urea cycle detoxification pathway (CPS1) of low-expression cancer types can effectively enhance the immune response. The establishment of innovative serum ammonia metabolism markers and the ultimate confirmation of GLS as the core hub integrating the three dimensions of metabolism, genomics and immunity have laid a theoretical foundation for tumor synergistic therapy targeting ammonia metabolism.

Keywords

Glutaminase gene, Ammonia death, Immune microenvironment, Metabolic-immune cross-regulation, Pan-cancer analysis

Introduction

Glutamine, recognized as the most prevalent free amino acid in the bloodstream, serves not only as a nitrogen donor for cellular biosynthesis but also as a critical metabolic hub for sustaining immune homeostasis [1]. Under physiological conditions, glutamine synthase (GS) catalyzes the conversion of glutamic acid and ammonia into glutamine, thereby providing essential energy for immune cells such as lymphocytes and macrophages, and participating in the urea cycle to regulate acid-base

balance [2]. However, within the tumor microenvironment (TME), this meticulously regulated metabolic network becomes significantly disrupted. Cancer cells enhance glutamine catabolism by overexpressing glutaminase (GLS), leading to an accumulation of ammonia [3]. The pioneering research conducted by Huang Bo’s team, published in *Nature Cell Biology* in 2024, unveiled a novel finding: Within the tumor microenvironment, CD8⁺ effector T cells release

mitochondrial ammonia because of enhanced glutamine catabolism. This release leads to lysosomal alkalization ($\text{pH} > 7.2$) and the collapse of mitochondrial membrane potential, culminating in the induction of a newly identified form of cell death termed “ammoniaptosis” [4]. Concurrently, memory T cells mitigate ammonia toxicity through the urea cycle detoxification pathway, facilitated by carbamoyl phosphate synthase-1 (CPS1) [5]. In contrast, the lack of CPS1 in effector T cells emerges as a critical factor contributing to immune dysfunction.

The GLS gene family (ENSG00000115419) is a central regulator of nitrogen metabolism, with the glutaminase it encodes facilitating the hydrolysis of glutamine into glutamic acid and ammonia. This reaction directly influences the ammonia metabolic flux within tumors [6]. While previous research has documented aberrant expression of GLS in certain cancer types, its potential role in altering the immune microenvironment via the “ammonia death” pathway across various cancers remains unclear. It is particularly important to investigate how GLS expression impacts the fate of CD8^+ T cells. Furthermore, what interactions exist between GLS expression, DNA damage repair mechanisms, and immune checkpoint expression? These issues hold substantial importance for advancing immunotherapy strategies that target ammonia metabolism. This study, through the construction of a cross-regulatory network encompassing “metabolism-genome-immunity”, not only addresses the theoretical gap concerning ammonia metabolism in tumor immune editing but also establishes a molecular foundation for the clinical development of synergistic therapies involving GLS inhibitors and immune checkpoint blockade.

Materials and Methods

This study utilizes the TCGA TARGET GTEx pan-cancer dataset from the UCSC database (PANCAN,

$N=19,131$, $G=60,499$) to systematically examine the expression characteristics and clinical significance of the GLS gene (ENSG00000115419) across various cancer types [7,8]. Initially, the expression matrix for the GLS gene was extracted, and samples were selected from primary tumors, blood-derived cancers, and metastatic sites. Zero-expression samples were excluded, and the expression values were subjected to a $\log_2(x+1)$ transformation for standardization. Cancer types with fewer than three samples were excluded, resulting in the retention of 26 to 44 different cancer types. Differential expression analysis was performed using the unpaired t-test to compare tumor samples with normal tissues, with a significance threshold set at $p < 0.05$.

Prognostic analysis was carried out by integrating clinical follow-up data from The Cancer Genome Atlas (TCGA) with the complementary prognostic dataset from TARGET [9]. Subsequently, a Cox proportional hazards regression model was constructed to evaluate risk factors, utilizing the R package survival (version 3.2-7) for statistical modeling [10]. Finally, the significance of differences in survival outcomes between defined groups was rigorously assessed through the Logrank test [11]. The immune microenvironment was analyzed using the ESTIMATE algorithm to calculate matrix and immune scores, and infiltration levels of 22 types of immune cells were quantified using TIMER, CIBERSORT, and five additional algorithms [12-14]. The correlation between GLS expression and immune characteristics was examined using the Pearson correlation test [15]. The genomic profiling analysis incorporated the TCGA Pan-cancer mutation data processed using MuTect2 and employed the maf-tools package [16,17]. Eight indicators, including tumor mutational burden (TMB) and loss of heterozygosity (LOH), were computed, and their associations with GLS expression were evaluated. All statistical analyses were conducted within the R 3.6.4 environment, with statistical significance

established at $p<0.05$.

Results and discussion

Differential expressions of GLS gene and prognosis analysis

In this study, the TCGA TARGET GTEx pan-cancer dataset (PANCAN, N=19,131) was utilized to construct a comprehensive expression map of the GLS gene across 26 cancer types (Figure 1). The findings indicate that GLS expression exhibits significant specificity to cancer type, with marked upregulation observed in nine cancer types, particularly within tumors of the digestive system. Notably, GLS expression was significantly elevated in esophageal carcinoma (ESCA) (tumor/normal: 5.47 ± 0.91 vs. 3.98 ± 1.24 , $p=9.5e-4$), stomach adenocarcinoma (STAD) (4.78 ± 0.92 vs. 3.68 ± 0.88 , $p=9.2e-9$), and cholangiocarcinoma (CHOL)

(4.93 ± 0.85 vs. 2.08 ± 0.34 , $p=2.8e-17$), with all differences exceeding a 1.5-fold increase. It is hypothesized that GLS-driven reprogramming of glutamine metabolism may constitute the central mechanism for energy supply in tumors of the digestive tract.

The expression of GLS was markedly downregulated across 13 cancer types, including glioma (GBM: 4.06 ± 0.60 compared to 6.57 ± 0.85 , $p=2.6e-3$) and urinary system tumors (KIRC: 6.30 ± 0.89 compared to 7.31 ± 0.63 , $p=1.0e-36$). This bidirectional regulatory model suggests that elevated GLS expression may facilitate T-cell ammonia-induced apoptosis via ammonia production, thereby contributing to the formation of an immune-evasive microenvironment. Conversely, reduced GLS expression may be linked to metabolic adaptations resulting from urea cycle deficiencies.

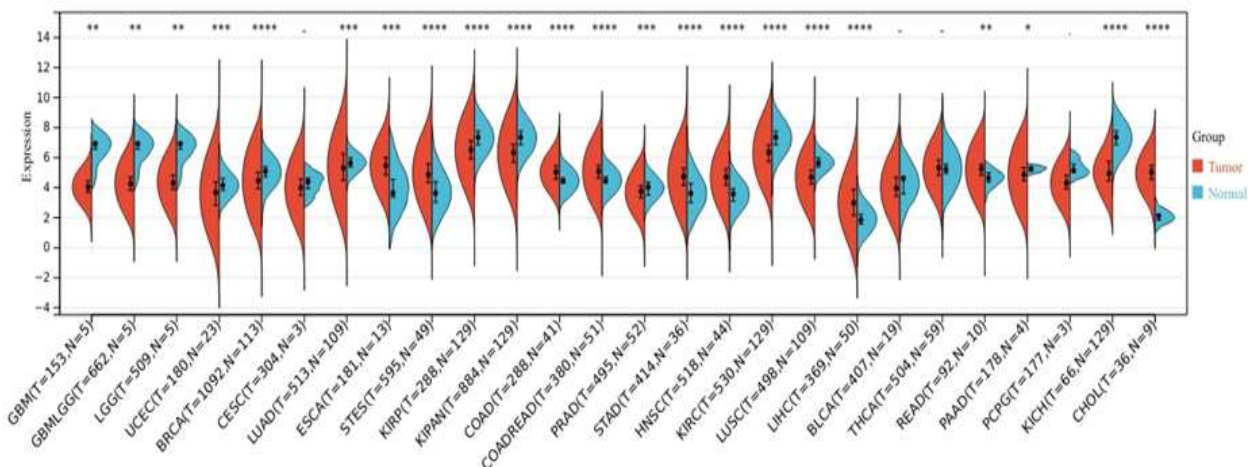


Figure 1. GLS gene pan-cancer differential expression atlas.

Figure 2-4 illustrates the intricate relationship between GLS expression and patient survival, as analyzed using the Cox proportional hazards model and Logrank test. In the TARGET-LAML cohort (acute myeloid leukemia, HR (Hazard Ratio)=1.28, $p=0.01$), TCGA-LIHC cohort (hepatocellular carcinoma, HR=1.28, $p=9.8e-4$), and TCGA-MESO cohort (mesothelioma, HR=1.44, $p=0.03$), elevated GLS expression is significantly associated with reduced overall survival.

This observation may be attributed to lysosomal

rupture and mitochondrial damage in CD8+T cells, potentially induced by ammonia accumulation, a process referred to as the ammonia death pathway. Conversely, in the TCGA-KIRC cohort (clear cell renal cell carcinoma, HR=0.80, $p=5.2e-3$), lower GLS expression correlates with poorer prognosis. This phenomenon may be linked to ammonia detoxification disorders resulting from the absence of the CPS1 enzyme, a finding that aligns with the protective mechanism of CPS1 identified by Huang Bo's research team.

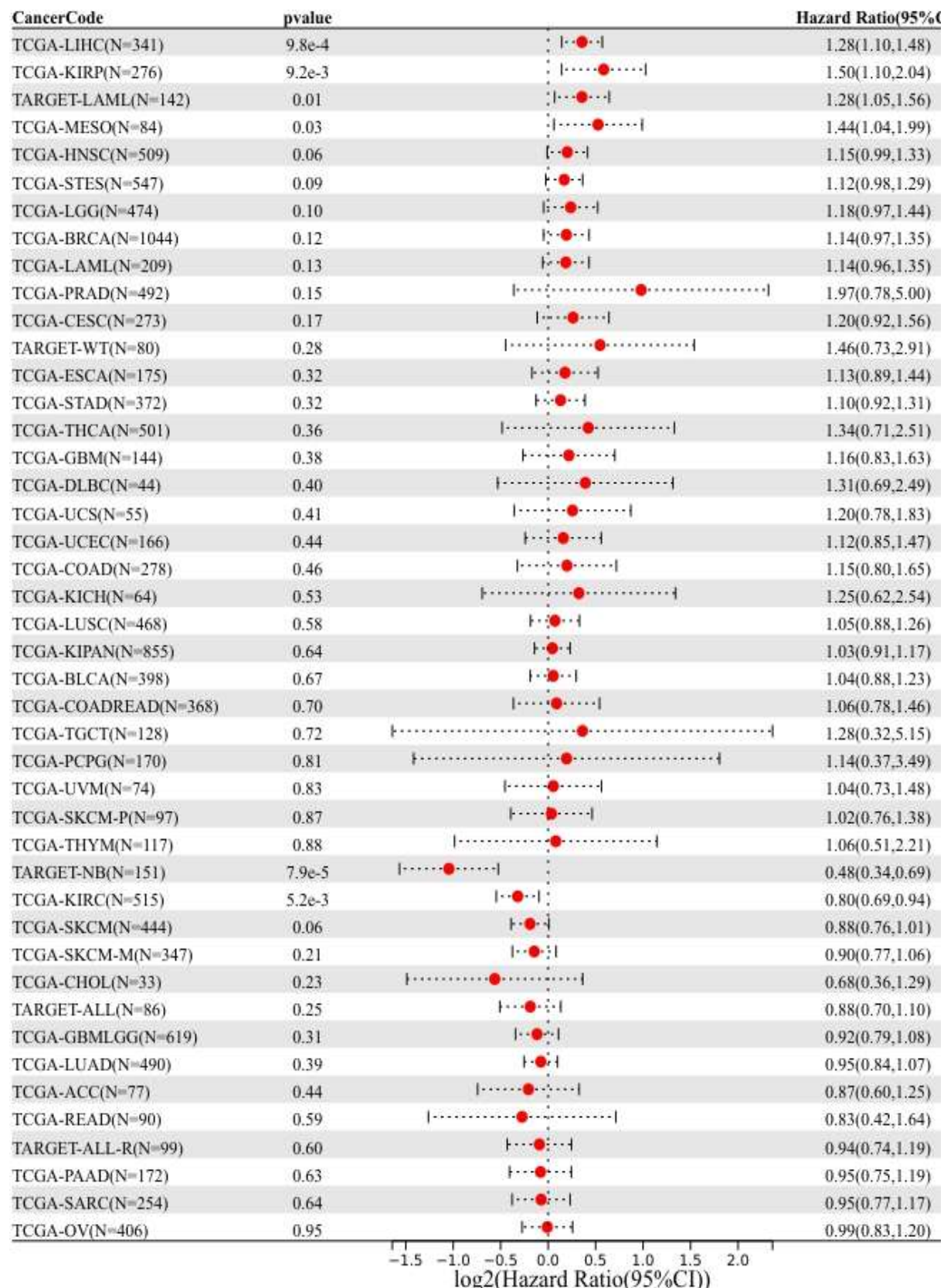


Figure 2. GLS expression level stratified survival curve.

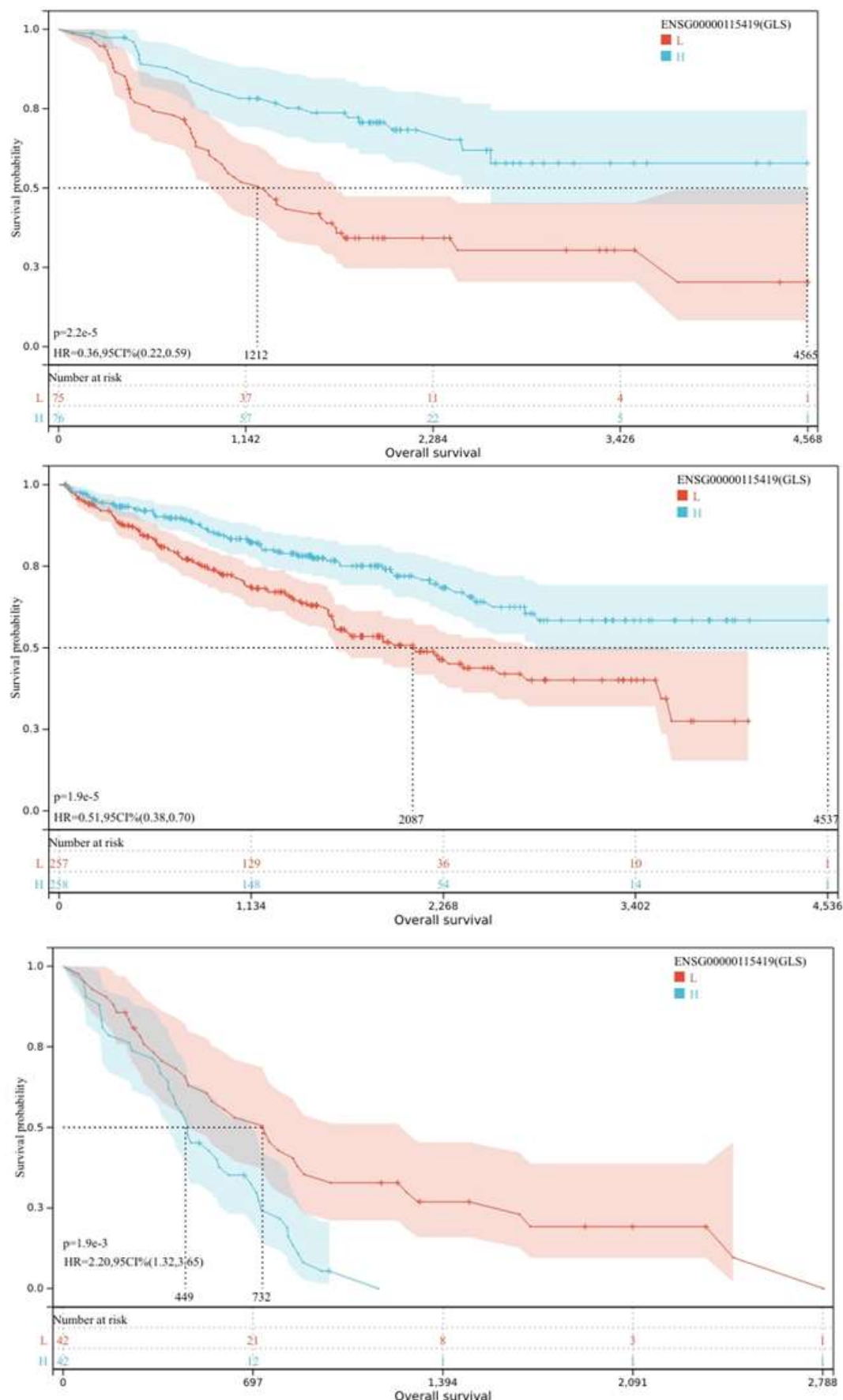


Figure 3. GLS expression prognostic risk model (abc).

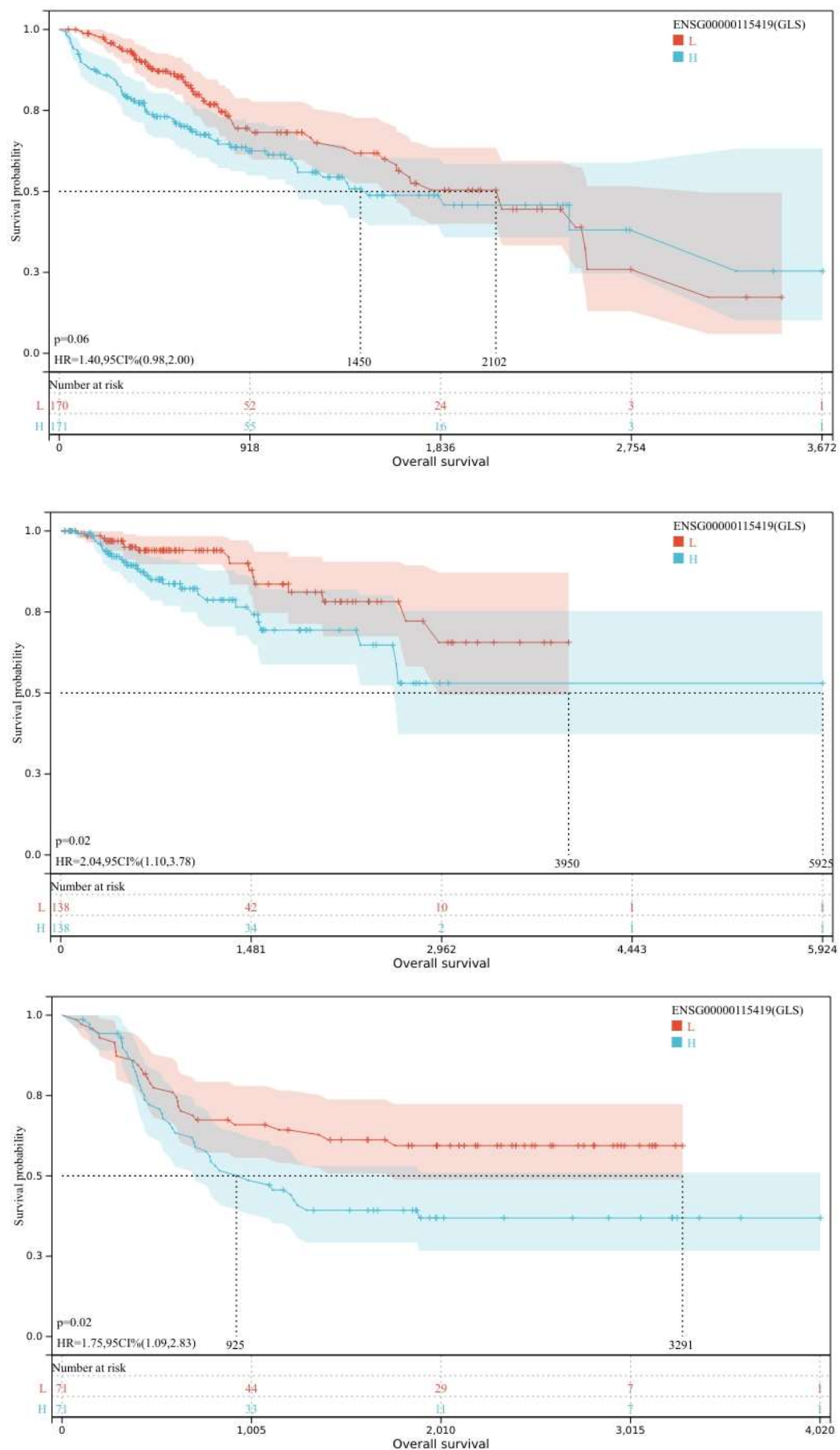


Figure 4. GLS expression prognostic risk model (def).

Figure 1-4 illustrates a U-shaped relationship between GLS expression and tumor biological behavior through joint analysis. Specifically, in the majority of solid tumors, GLS overexpression promotes cancer cell proliferation via the metabolic conversion of glutamine to glutamic acid and subsequently to α -ketoglutarate. Concurrently, the ammonia released in this process induces T cell apoptosis within the tumor microenvironment. Conversely, in certain cancer types, low GLS expression results in impaired ammonia detoxification. This impairment activates the p38MAPK/JNK signaling pathway, leading to genomic instability [18]. These findings provide a theoretical foundation for the development of precise GLS-targeted therapies: GLS inhibitors could be effective for cancers with high GLS expression, whereas CPS1 activators might be necessary to restore ammonia metabolism in cancers with low GLS expression. This study is pioneering in linking the “ammonia death” mechanism to pan-cancer prognosis, thereby offering a novel perspective for research at the intersection of metabolism and immunology

GLS genomic heterogeneity and gene expression analysis

This study conducted a systematic analysis of the relationship between GLS expression and eight core genomic characteristic indicators by integrating data from the TCGA Pan-cancer dataset (N=10,535) (Figure 5-8). Among the 37 cancer types examined, GLS expression exhibited a significant negative correlation with tumor mutational burden (TMB), particularly in cholangiocarcinoma (CHOL, $r= -0.51$, $p=0.002$) and gastrointestinal cancers (STAD, $r= -0.12$, $p=0.02$; COADREAD, $r= -0.11$, $p=0.03$). This finding suggests that elevated GLS expression may inhibit mutation accumulation or be associated with the maintenance of DNA repair pathway activity through glutamine metabolism. Additionally, GLS expression was significantly positively correlated with the tumor heterogeneity indicator MATH in seven cancer types, including STES ($r=0.18$, $p=7.2e-7$) and COAD ($r=0.19$, $p=0.001$), indicating that GLS-driven ammonia

production may enhance subclonal diversity by inducing mitochondrial stress responses. Furthermore, the study identified a bidirectional regulation of microsatellite instability (MSI) with GLS expression, demonstrating a positive correlation in glioma (GBMLGG, $r=0.17$, $p=1.7e-5$) and renal cell carcinoma (KIRC, $r=0.13$, $p=0.02$) [19]. In diffuse large B-cell lymphoma (DLBC, $r= -0.50$, $p=0.0003$) and colorectal cancer (COAD, $r= -0.20$, $p=0.0007$), a negative correlation was observed. This differentiation phenomenon underscores tissue specificity, indicating that in cancer types with high microsatellite instability (MSI), glutaminase (GLS) may influence genomic stability by modulating the expression of mismatch repair (MMR) genes. Additionally, neo-antigen loading (Neo) exhibited a positive correlation with GLS in glioblastoma (GBM, $r=0.21$, $p=0.046$), whereas a negative correlation was noted in cholangiocarcinoma (CHOL, $r= -0.46$, $p=0.02$). These findings suggest that the expression level of GLS may indirectly regulate T-cell responses by altering tumor immunogenicity.

Regarding the characteristics of the tumor microenvironment, GLS demonstrated a significant negative correlation with tumor purity across 15 cancer types. Notably, in hepatocellular carcinoma (LIHC, $r= -0.18$, $p=0.0008$) and bladder cancer (BLCA, $r= -0.26$, $p=1.8e-7$), this correlation indirectly supports its potential role in promoting stromal remodeling. Conversely, a positive correlation with tumor ploidy was observed in gastrointestinal cancer (STES, $r=0.21$, $p=3.2e-7$) and endometrial cancer (UCEC, $r=0.22$, $p=0.003$), suggesting that elevated GLS expression may contribute to chromosomal instability. Loss of heterozygosity (LOH) exhibited a strong positive correlation with GLS across 12 cancer types, including breast cancer (BRCA, $r=0.28$, $p=2.3e-20$) and liver hepatocellular carcinoma (LIHC, $r=0.34$, $p=2.8e-11$). Additionally, homologous recombination deficiency (HRD) showed a positive correlation in 9 cancer types, implying GLS may disrupt DNA damage repair via ammonia toxicity and amplify genomic vulnerability. This finding

establishes a molecular feedback loop with the earlier “ammonia death” mechanism, which

disrupts cellular homeostasis by destabilizing the lysosome-mitochondrial axis.

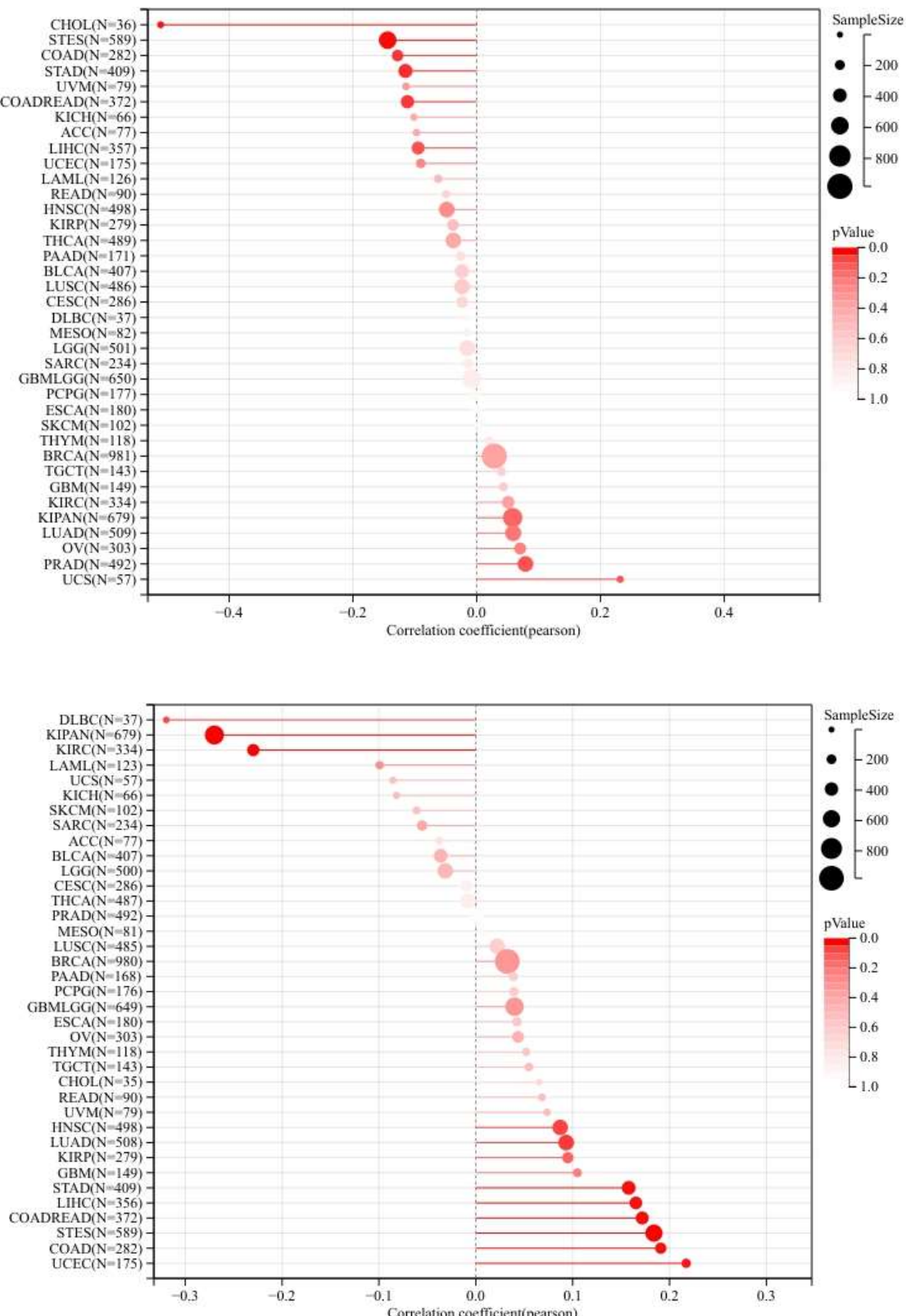


Figure 5. Network of the relationship between GLS expression and genomic instability in TMB and MATH.

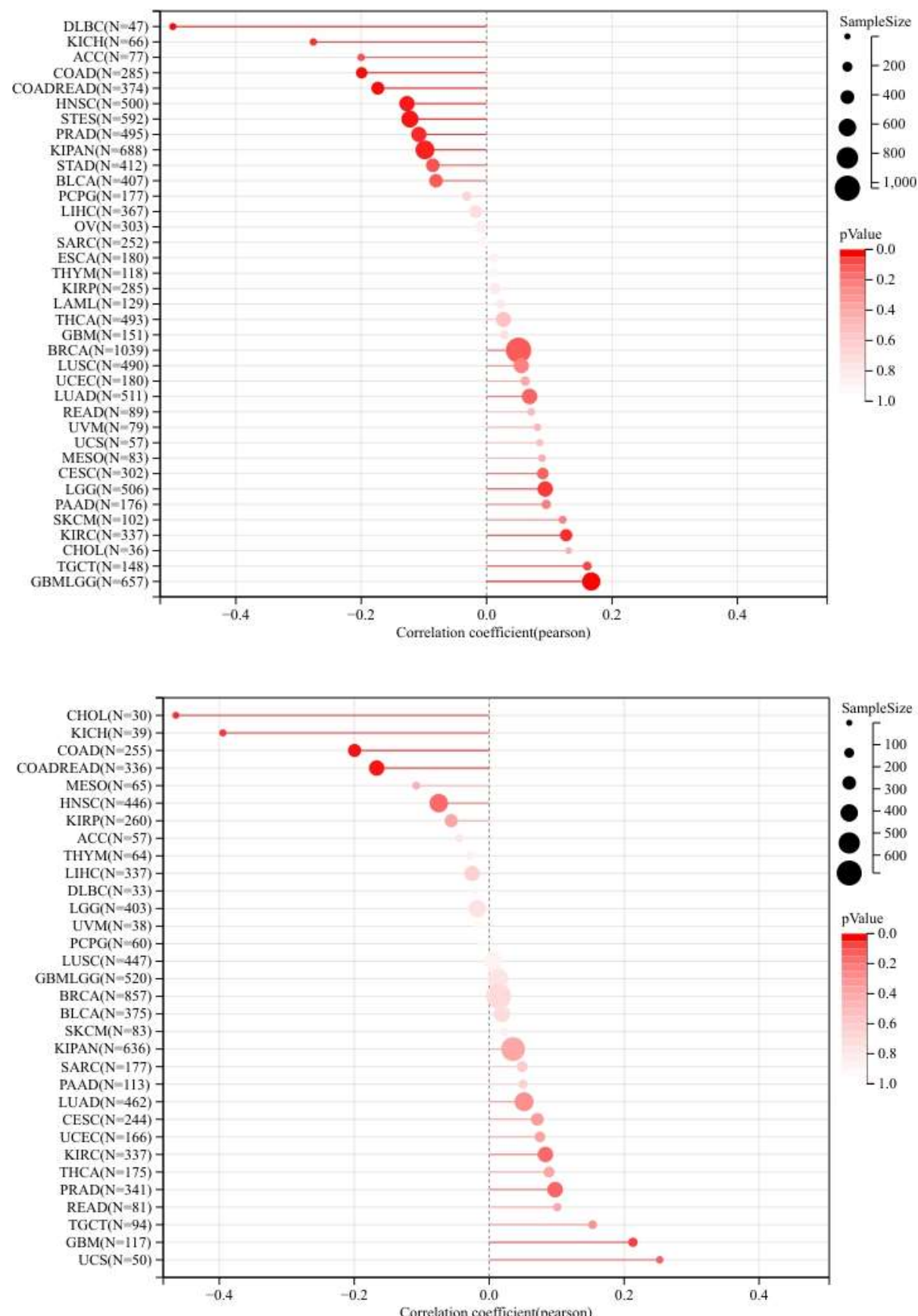


Figure 6. Network of the relationship between GLS expression and genomic instability in MSI and NEO.

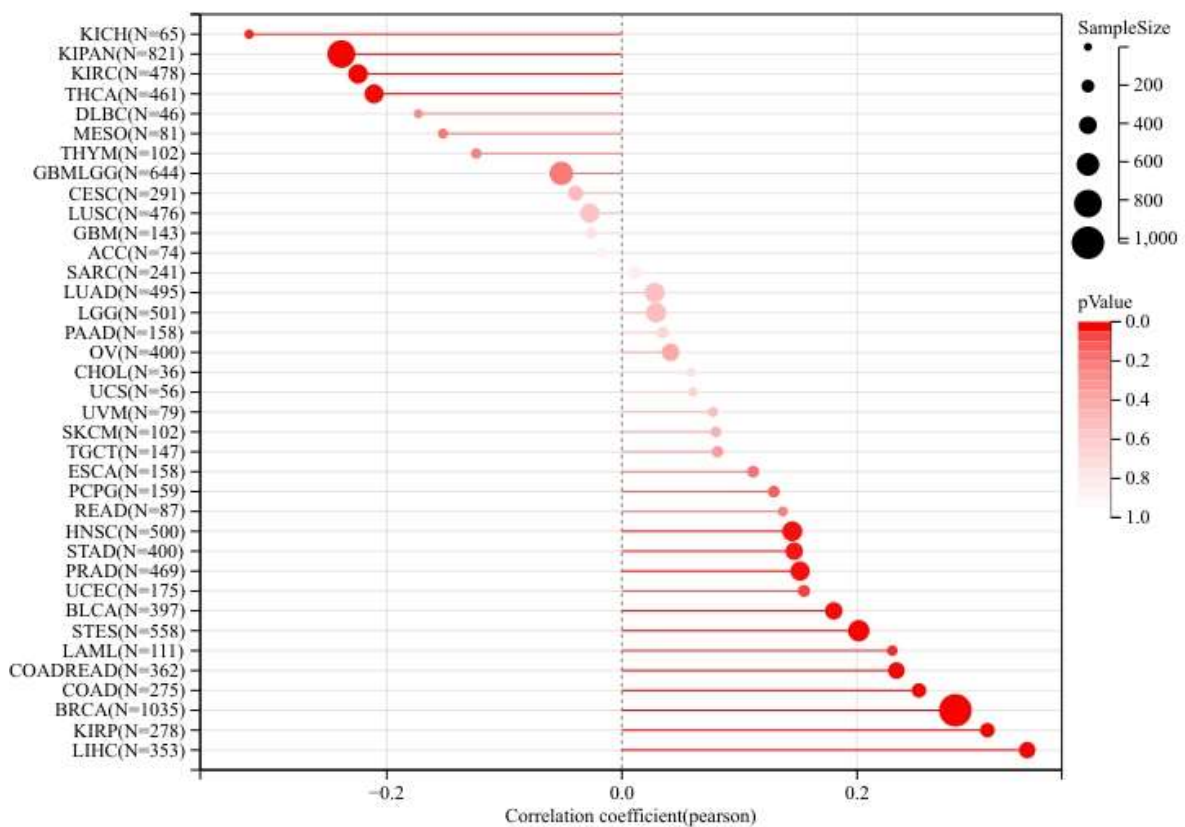
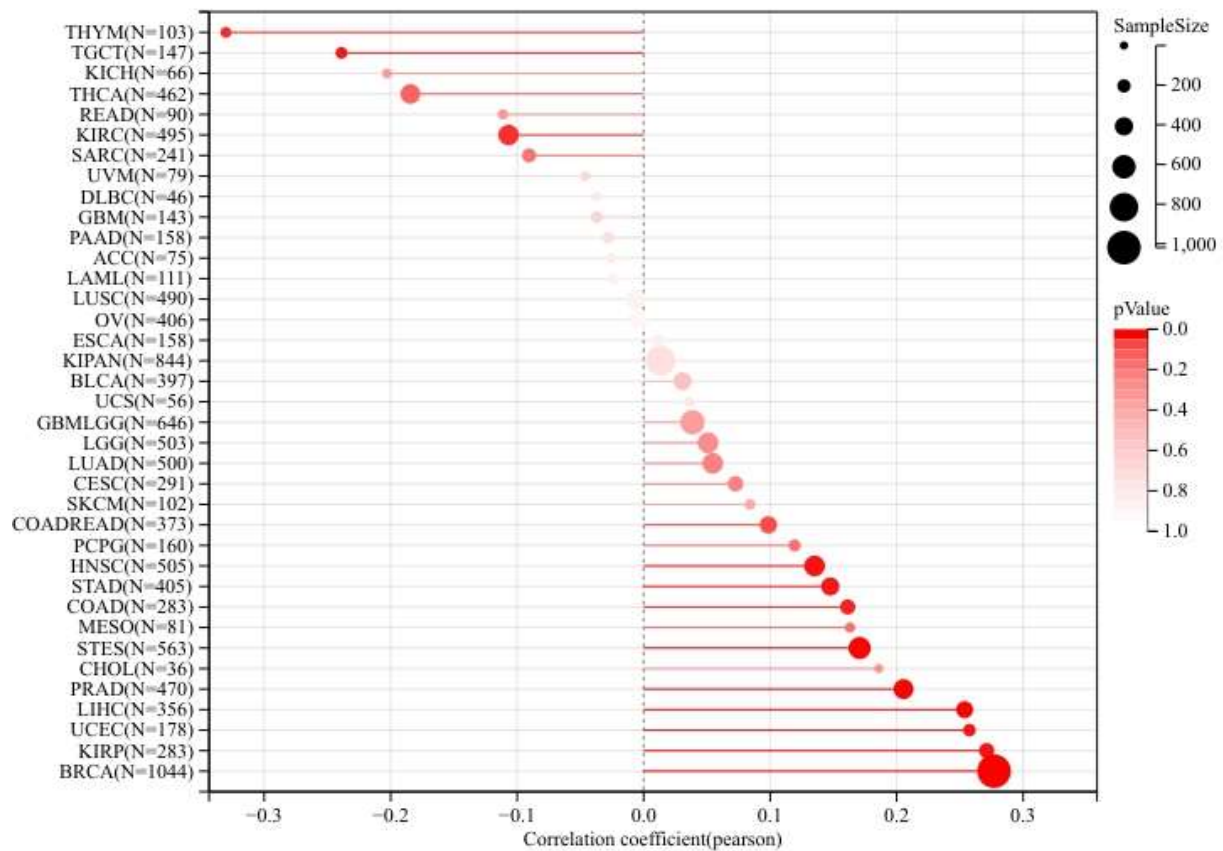


Figure 7. Network of the relationship between GLS expression and genomic instability in HRD and LOH.

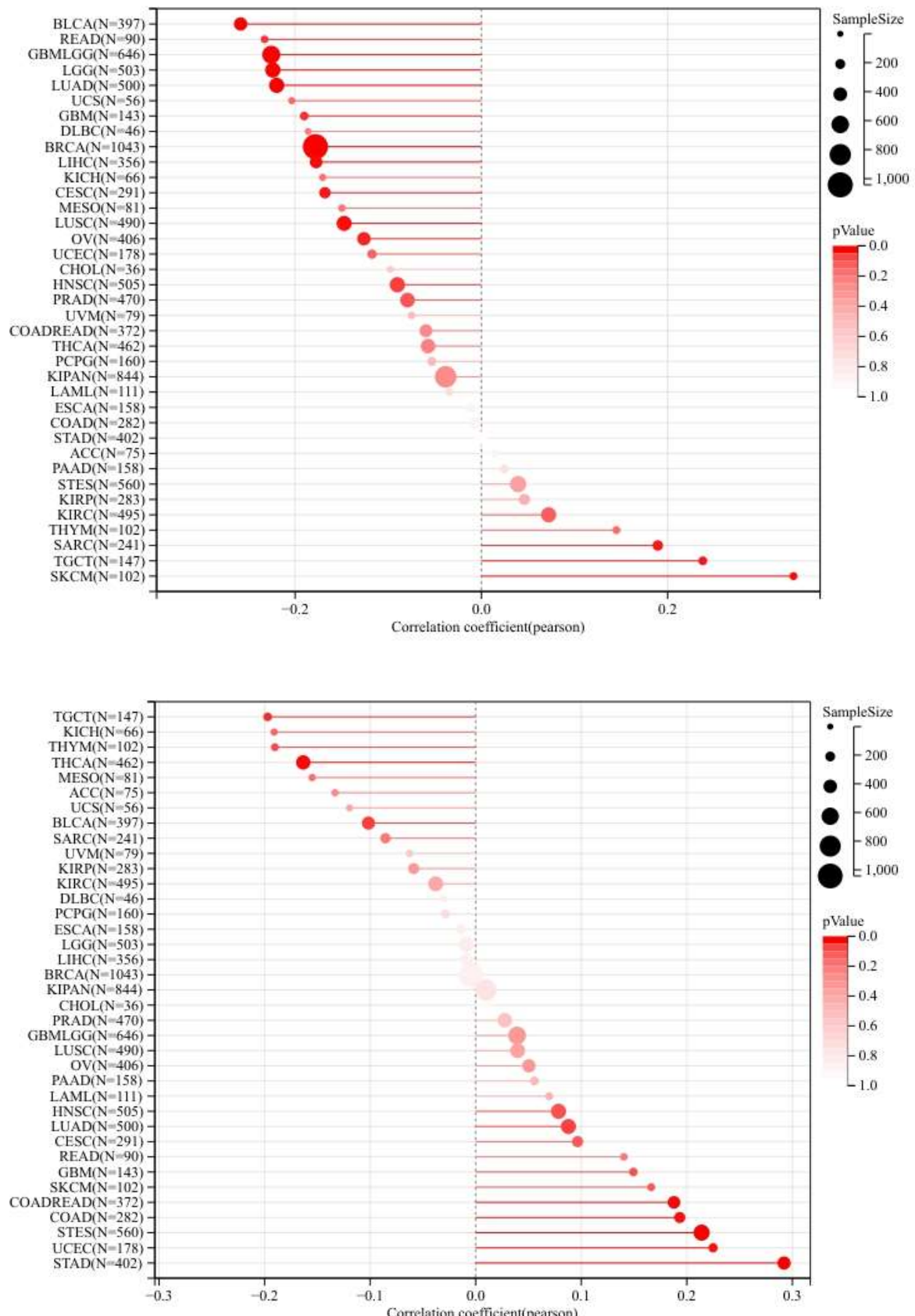


Figure 8. Network of the relationship between GLS expression and genomic instability in Purity and Ploidy.

Immune microenvironment analysis

This study elucidated the bidirectional regulatory role of GLS on immune checkpoints through a systematic analysis of the correlation between GLS expression and 60 key immune checkpoint genes, comprising 24 inhibitory and 36 stimulatory genes, using the Pearson correlation test ($p<0.05$) (Figure 9). Across 18 cancer types, including TCGA-BRCA ($N=1077$) and TCGA-LUAD ($N=500$), a significant positive correlation was observed between GLS expression and immune checkpoints. Notably, PD-L1 (CD274) exhibited the strongest correlation in digestive tract tumors, specifically in STAD ($r=0.31$, $p<1e-5$), suggesting that elevated GLS expression may facilitate the upregulation of immune

checkpoints and contribute to T cell exhaustion via activation of the Hippo-YAP pathway [20]. Nevertheless, a negative correlation was observed in glioma (TCGA-GBMLGG, $R=-0.17$, $p=1.5e-5$) and metastatic melanoma (TCGA-SKCM-M, $R=-0.29$, $p=3.8e-3$). This phenomenon may be attributed to the compensatory upregulation of inhibitory checkpoints such as IDO1 and VISTA, which is triggered by the low expression of GLS [21]. This tissue-specific pattern suggests that GLS can modulate immune microenvironment balance via the "metabolism-immune checkpoint axis," promoting depletion phenotypes at high expression and inducing immunosuppression when expression is low.

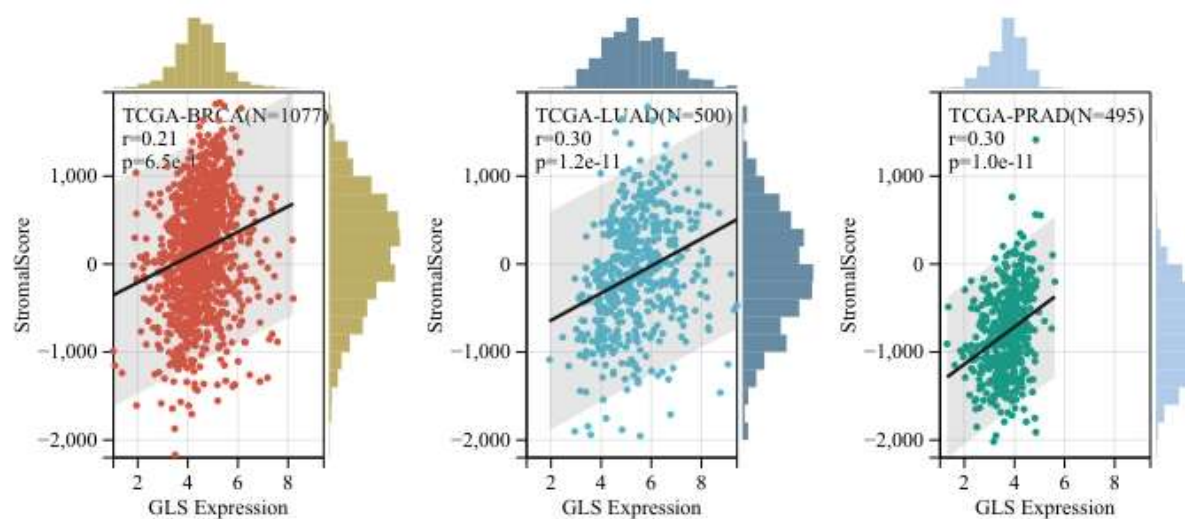


Figure 9. Pan-cancer regulatory network of GLS expression and immune checkpoint genes.

Utilizing seven immune infiltration quantification algorithms, including ESTIMATE, TIMER, and CIBERSORT, alongside immune checkpoint gene analysis, Figure 10-16 provides a comprehensive overview of the relationship between GLS expression and immune cell infiltration across 10,179 samples spanning 44 cancer types. The ESTIMATE algorithm revealed that GLS significantly influenced the immune score in 22 cancer types. Notably, BRCA ($r=0.21$, $p=6.5e-12$) and LUAD ($r=0.30$, $p=1.2e-11$) exhibited a strong positive correlation, underscoring GLS's role in facilitating the recruitment of immune cells. The

integrated analysis of multiple computational algorithms demonstrated that both the CIBERSORT and Xcell algorithms consistently identified elevated expression levels of GLS in digestive system cancers, specifically stomach adenocarcinoma (STAD) and colon adenocarcinoma (COAD). This was associated with increased infiltration of CD8+T cells ($r=0.33$, $p<1e-6$) and M1-type macrophages ($r=0.28$, $p<0.001$). These findings suggest that the GLS gene may activate the HIF-1 α pathway via the glutamine metabolite α -KG. Conversely, the TIMER and QUANTISEQ algorithms indicated that in renal cell

carcinoma (KIRC), reduced GLS expression was correlated with enhanced neutrophil infiltration ($R=-0.41$, $p=8e-5$) [22]. Notably, the MCPCounter algorithm identified a negative correlation between high GLS expression and cytotoxic lymphocyte

infiltration in acute myeloid leukemia (LAML) ($R=-0.29$, $p=5.3e-4$) and skin cutaneous melanoma (SKCM) ($R= -0.29$, $p=3.8e-3$). This evidence directly supports the existence of the “GLS-ammonia death-CD8+ T cell exhaustion” axis.

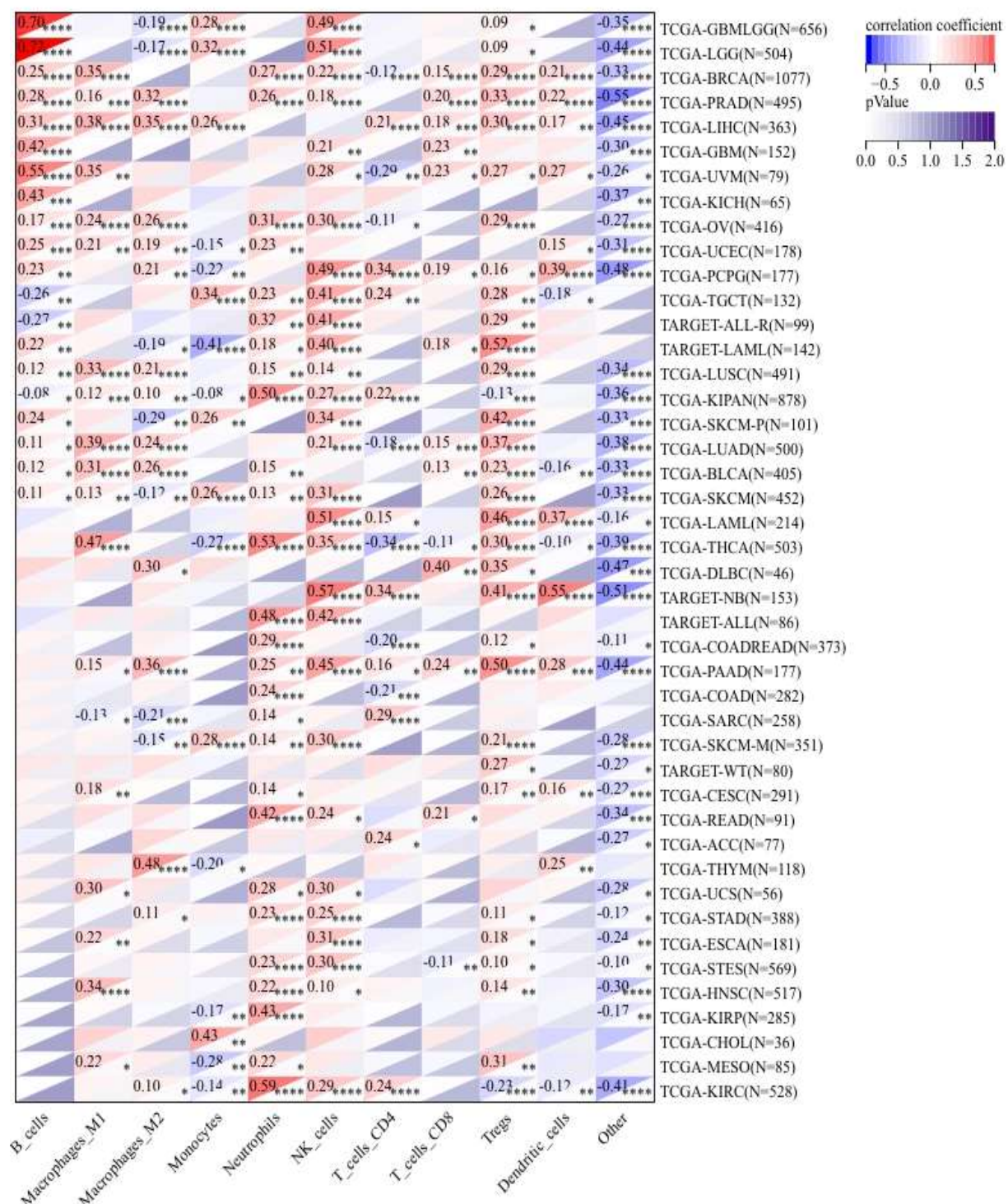


Figure 10. QUANTISEQ analysis of the immune cell infiltration pattern mediated by GLS.

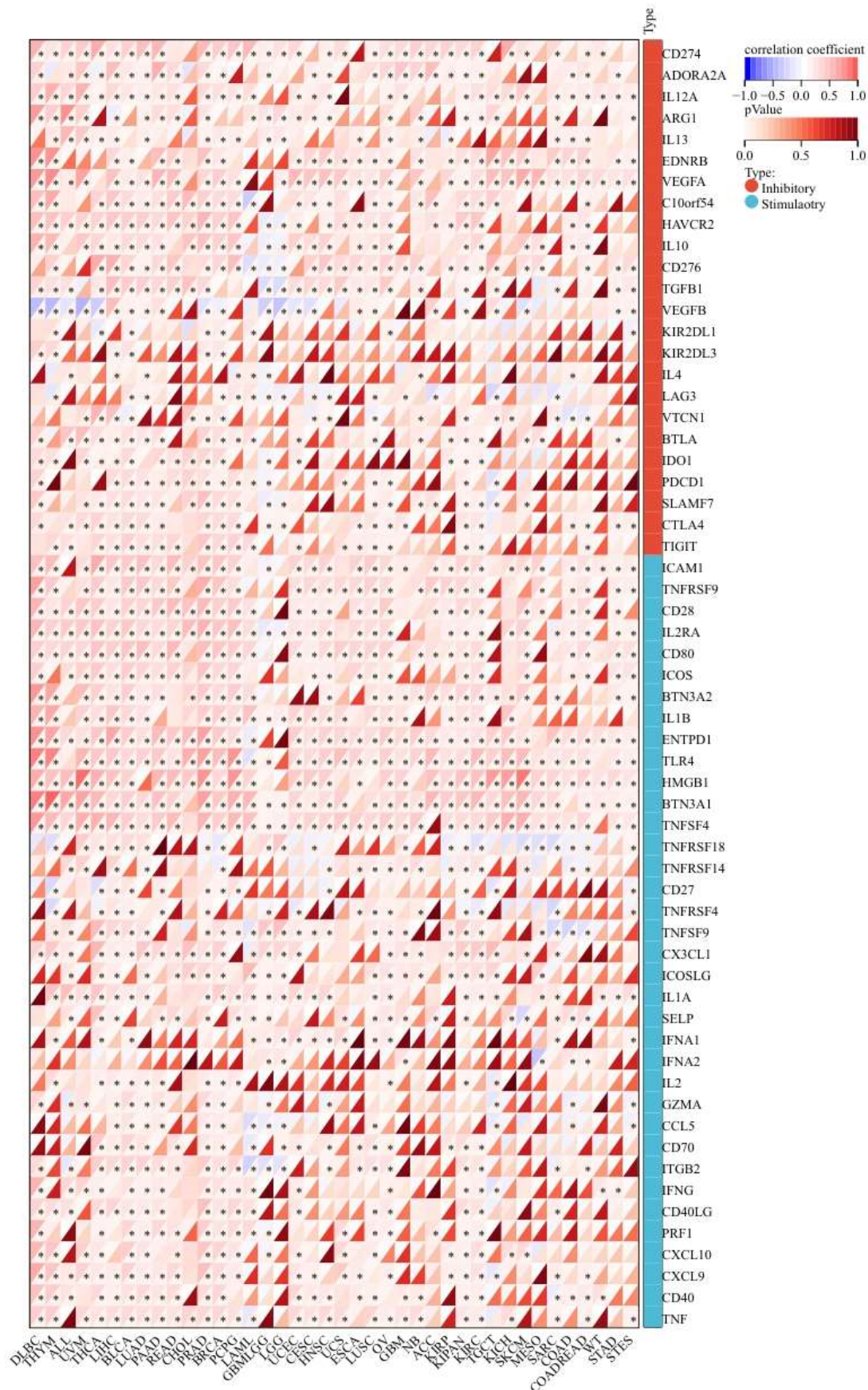


Figure 11. Analysis of immune checkpoint genes.

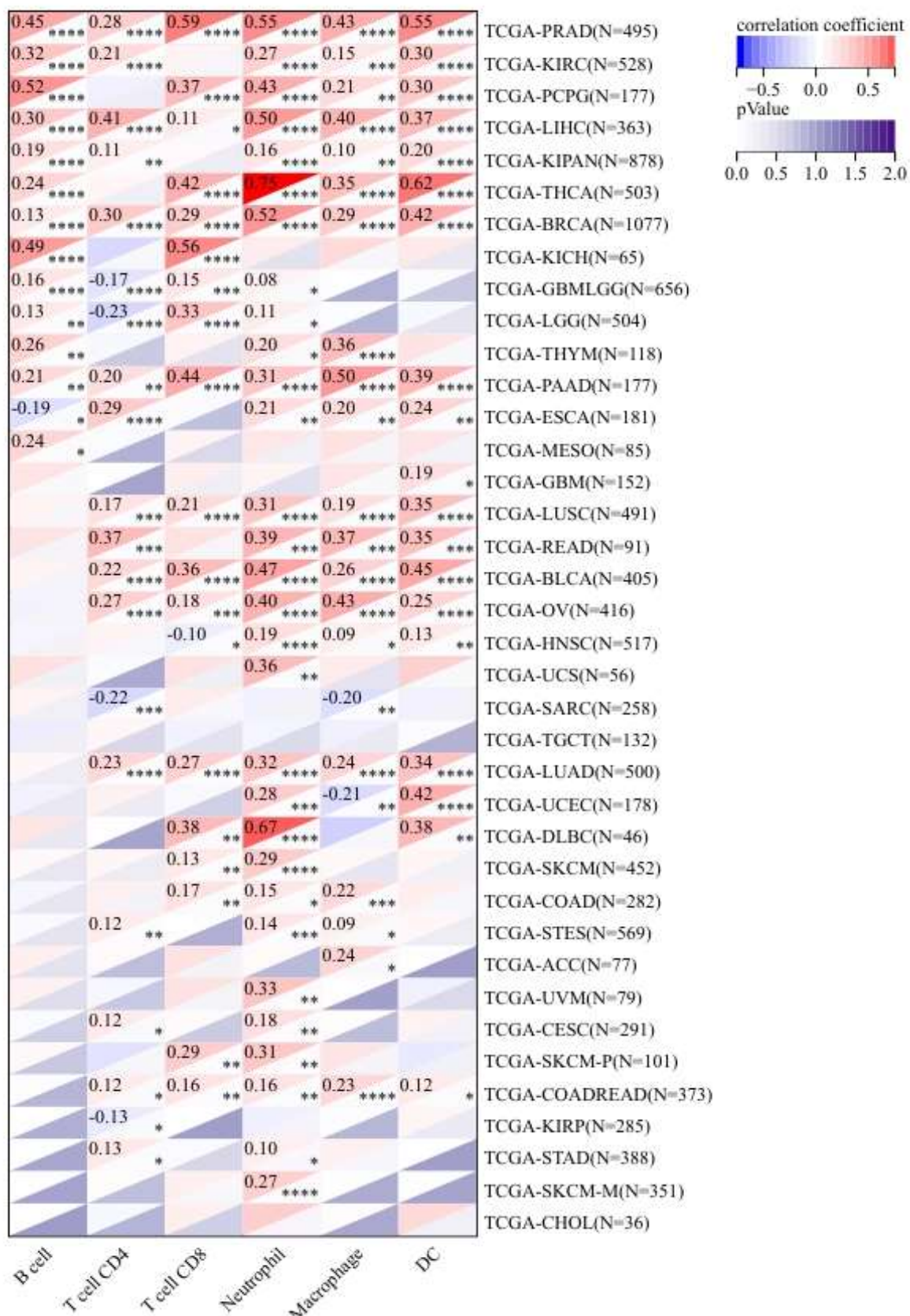


Figure 12. TIMBER analysis of the immune cell infiltration pattern mediated by GLS

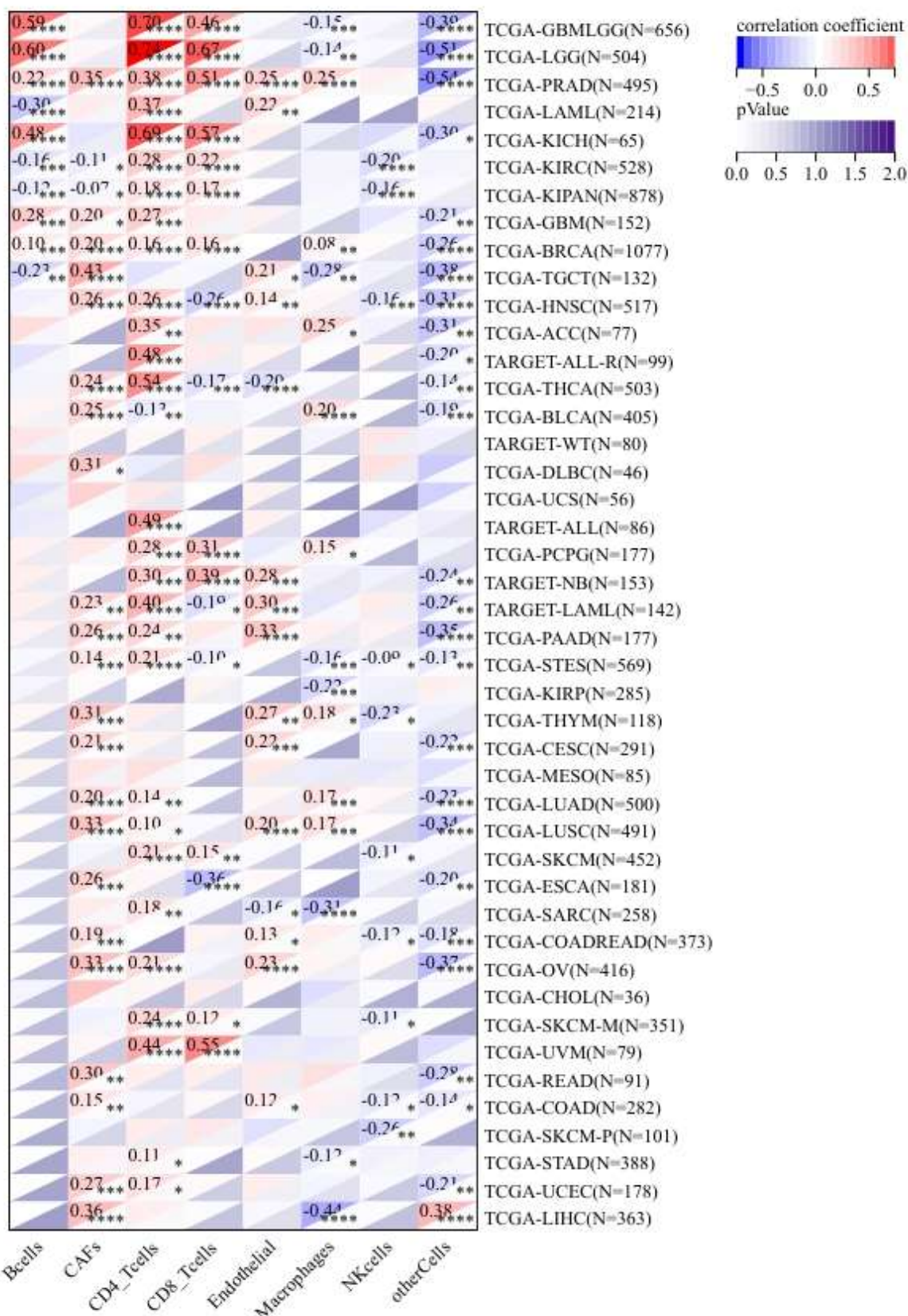


Figure 13. EPIC analysis of the immune cell infiltration pattern mediated by GLS.

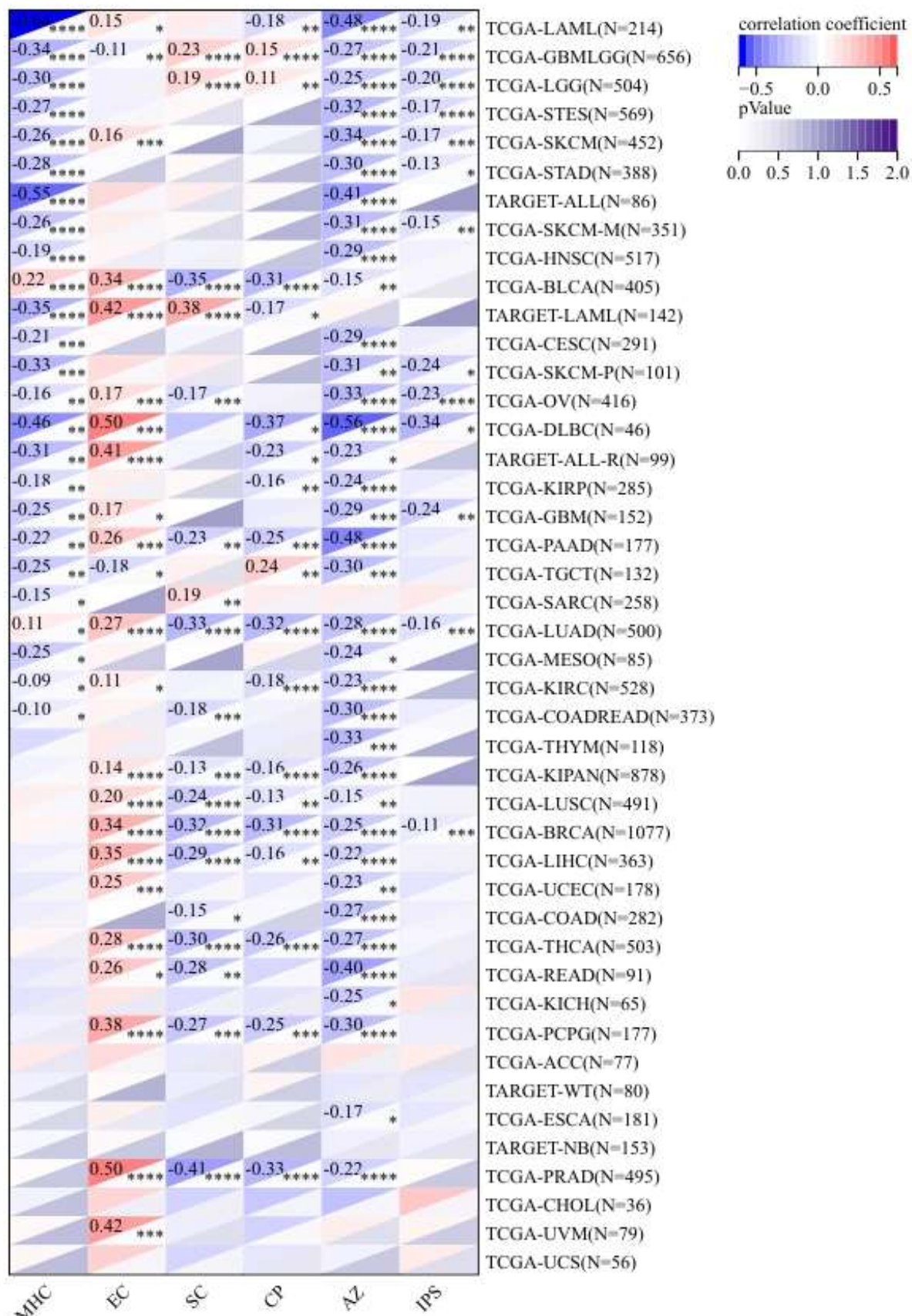


Figure 14. IPS analysis of the immune cell infiltration pattern mediated by GLS.

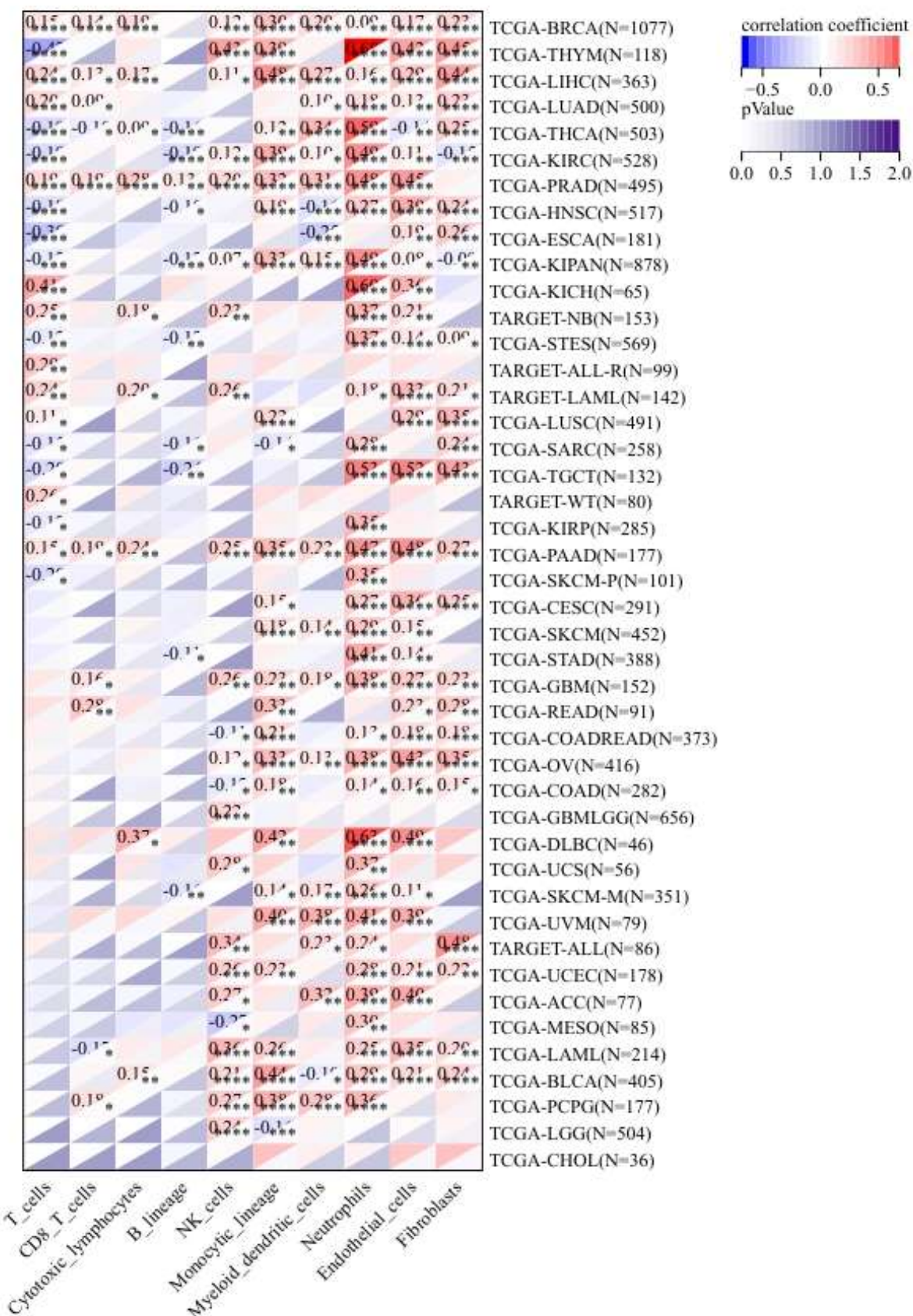


Figure 15. MCPC counter analysis of the immune cell infiltration pattern mediated by GLS.

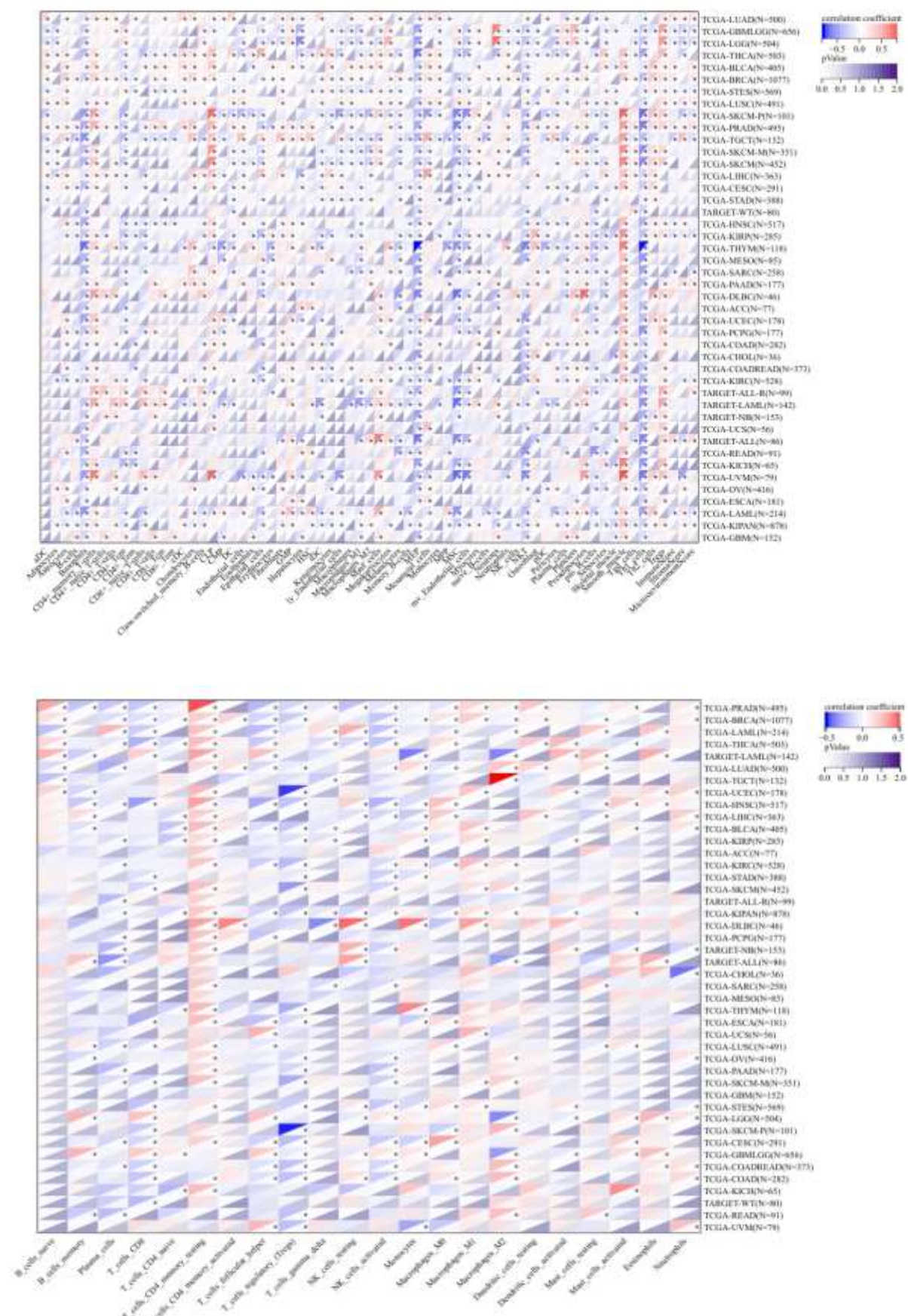


Figure 16. CIBERSORT and Xcell analysis of the immune cell infiltration pattern mediated by GLS.

Conclusion

In this study, we conduct a comprehensive analysis of the multi-dimensional regulatory network of the GLS gene within tumor biology by integrating extensive Pan-cancer datasets, including TCGA, TARGET, and GTEx, for the first time. At the expression level, GLS demonstrates significant tissue-specific heterogeneity. Its general upregulation in tumors of the digestive system and hematological malignancies is directly linked to the reprogramming of glutamine metabolism. Conversely, its downregulation in gliomas and renal cell carcinomas indicates cancer type-specific adaptive remodeling of ammonia metabolism pathways. Prognostic analysis further underscores the intricate clinical implications of GLS expression: elevated expression is associated with poor prognosis in hepatocellular carcinoma and mesothelioma, whereas reduced expression in clear cell renal cell carcinoma is indicative of decreased survival, thereby affirming the tissue-specific nature of the “GLS expression - ammonia accumulation - cell death” threshold. In the context of genomic stability, GLS modulates the tumor’s evolutionary trajectory through a metabolism-epigenetic interplay. Notably, high GLS expressions significantly reduce the mutational burden in gastrointestinal cancers yet exacerbate the loss of heterozygosity by inducing lysosomal alkalization. This ostensibly paradoxical phenomenon unveils a novel mechanism of DNA repair imbalance mediated by ammonia toxicity, wherein ammonia overload in the microenvironment inhibits ATR kinase activity, consequently impairing the efficacy of homologous recombination repair. Within the context of the immune microenvironment, glutaminase (GLS) demonstrates a dual effect. It facilitates immune recognition by enhancing antigen presentation through the production of α -ketoglutaric acid. However, an excessive accumulation of ammonia can lead to the disruption of mitochondrial membrane potential in CD8+ T cells, activating the ammonia-induced cell death pathway.

The primary translational significance of this study

is the development of the inaugural “metabolism-immunity” precision intervention framework. For cancer types characterized by GLS overexpression, the application of GLS inhibitors can decrease ammonia concentrations within the microenvironment, thereby alleviating T cell exhaustion and enhancing the response rate to PD-1 antibodies. Conversely, in cancer types with low GLS expression, the activation of the urea cycle rate-limiting enzyme CPS1 can reconstruct the ammonia detoxification barrier and augment CD8+ T cell infiltration. These findings not only broaden the applicability of the “ammonia death” mechanism across various cancer types but also position GLS as a central node integrating the domains of metabolism, genomics, and immunity.

Funding

This work was not supported by any funds.

Acknowledgements

The authors would like to show sincere thanks to those techniques who have contributed to this research.

Conflicts of Interest

The authors declare no conflicts of interest.

References

- [1] Cruzat, V., Macedo Rogero, M., Noel Keane, K., Curi, R., Newsholme, P. (2018) Glutamine: metabolism and immune function, supplementation and clinical translation. *Nutrients*, 10(11), 1564.
- [2] Weiner, I. D., Verlander, J. W. (2017) Ammonia transporters and their role in acid-base balance. *Physiological Reviews*, 97(2), 465-494.
- [3] Li, D., Cao, D., Zhang, Y., Yu, X., Wu, Y., Jia, Z., Jiang, Z., Cao, X. (2025) Integrative pan-cancer analysis and experiment validation identified GLS as a biomarker in tumor progression, prognosis, immune microenvironment, and immunotherapy. *Scientific Reports*, 15(1), 525.
- [4] Zhang, H., Liu, J., Yuan, W., Zhang, Q., Luo, X., Li, Y., Peng, Y., Feng, J., Liu, X., Chen, J.,

Zhou, Y., Lv, J., Zhou, N., Ma, J., Tang, K., Huang, B. (2024) Ammonia-induced lysosomal and mitochondrial damage causes cell death of effector CD8+ T cells. *Nature Cell Biology*, 26(11), 1892-1902.

[5] Luo, Y., Zhang, S., Xie, H., Su, Q., He, S., Lei, Z. (2023) Prognosis and immunotherapy significances of a cancer-associated fibroblasts-related gene signature in lung adenocarcinoma. *Cellular and Molecular Biology*, 69(14), 51-61.

[6] Saha, S. K., Islam, S. R., Abdullah-Al-Wadud, M., Islam, S., Ali, F., Park, K. S. (2019) Multiomics analysis reveals that GLS and GLS2 differentially modulate the clinical outcomes of cancer. *Journal of Clinical Medicine*, 8(3), 355.

[7] Lee, C. M., Barber, G. P., Casper, J., Clawson, H., Diekhans, M., Gonzalez, J. N., Kent, W. J. (2020) UCSC Genome Browser enters 20th year. *Nucleic Acids Research*, 48(D1), D756-D761.

[8] Chen, F., Fan, Y., Liu, X., Zhang, J., Shang, Y., Zhang, B., Tan, K. (2022) Pan-cancer integrated analysis of HSF2 expression, prognostic value and potential implications for cancer immunity. *Frontiers in Molecular Biosciences*, 8, 789703.

[9] Cappell, K. M., Kochenderfer, J. N. (2023) Long-term outcomes following CAR T cell therapy: What we know so far. *Nature Reviews Clinical Oncology*, 20(6), 359-371.

[10] Austin, P. C., Fang, J., Lee, D. S. (2022) Using fractional polynomials and restricted cubic splines to model non - proportional hazards or time - varying covariate effects in the Cox regression model. *Statistics in Medicine*, 41(3), 612-624.

[11] Royston, P., Choodari-Oskooei, B., Parmar, M. K., Rogers, J. K. (2019) Combined test versus logrank/Cox test in 50 randomised trials. *Trials*, 20(1), 172.

[12] Yoshihara, K., Shahmoradgoli, M., Martínez, E., Végesna, R., Kim, H., Torres-Garcia, W., Treviño, V., Shen, H., Laird, P. W., Levine, D. A., Carter, S. L., Getz, G., Stemke-Hale, K., Mills, G. B., Verhaak, R. G. (2013) Inferring tumour purity and stromal and immune cell admixture from expression data. *Nature Communications*, 4(1), 2612.

[13] Li, T., Fan, J., Wang, B., Traugh, N., Chen, Q., Liu, J. S., Li, B., Liu, X. S. (2017) TIMER: a web server for comprehensive analysis of tumor-infiltrating immune cells. *Cancer Research*, 77(21), e108-e110.

[14] Newman, A. M., Liu, C. L., Green, M. R., Gentles, A. J., Feng, W., Xu, Y., Alizadeh, A. A. (2015) Robust enumeration of cell subsets from tissue expression profiles. *Nature Methods*, 12(5), 453-457.

[15] Akoglu, H. (2018) User's guide to correlation coefficients. *Turkish Journal of Emergency Medicine*, 18(3), 91-93.

[16] Beroukhim, R., Mermel, C. H., Porter, D., Wei, G., Raychaudhuri, S., Donovan, J., Barretina, J., Boehm, J. S., Dobson, J., Urashima, M., Mc Henry, K. T., Pinchback, R. M., Ligon, A. H., Cho, Y. J., Haery, L., Greulich, H., Reich, M., Winckler, W., Meyerson, M. (2010) The landscape of somatic copy-number alteration across human cancers. *Nature*, 463(7283), 899-905.

[17] Jiang, F., Wu, C., Wang, M., Wei, K., Zhou, G., Wang, J. (2020) Multi-omics analysis of tumor mutation burden combined with immune infiltrates in melanoma. *Clinica Chimica Acta*, 511, 306-318.

[18] Wang, S. Y., Ni, X., Hu, K. Q., Meng, F. L., Li, M., Ma, X. L., Meng, T. T., Wu, H. H., Ge, D., Zhao, J., Li, Y., Su, G. H. (2020) Cilostazol alleviate nicotine induced cardiomyocytes hypertrophy through modulation of autophagy by CTSB/ROS/p38MAPK/JNK feedback loop. *International Journal of Biological Sciences*, 16(11), 2001.

[19] Zhu, J., Wang, J., Liu, H., Lei, T., Yang, J., Lan, S., Jian, H., Fang, H., Zhang, Y., Ren, K., Zhong, F. (2023) Crosstalk of cuproptosis-related prognostic signature and competing endogenous RNAs regulation in

hepatocellular carcinoma. *Aging (Albany NY)*, 15(23), 13901-13919.

[20] Ibar, C., Irvine, K. D. (2020) Integration of Hippo-YAP signaling with metabolism. *Developmental Cell*, 54(2), 256-267.

[21] Zhang, Y., Zheng, J. (2020) Functions of immune checkpoint molecules beyond immune evasion. *Regulation of Cancer Immune Checkpoints: Molecular and Cellular Mechanisms and Therapy*, 201-226.

[22] Zheng, J., Chen, P., Zhong, J., Cheng, Y., Chen, H., He, Y., Chen, C. (2021) HIF-1 α in myocardial ischemia-reperfusion injury. *Molecular Medicine Reports*, 23(5), 352.